

Antiproliferative effect of β -escin — an *in vitro* study

Gabriela Mojžišová¹✉, Martin Kello², Martina Pilátová², Vladimíra Tomečková³, Janka Vašková³, Ladislav Vaško³, Silvia Bernátová², Ladislav Mirossay² and Ján Mojžiš²

¹Department of Experimental Medicine, Faculty of Medicine, P. J. Šafárik University, 040 11 Košice, Slovak Republic; ²Department of Pharmacology, Faculty of Medicine, P. J. Šafárik University, 040 11 Košice, Slovak Republic; ³Department of Medical and Clinical Biochemistry, Faculty of Medicine, P. J. Šafárik University, 040 11 Košice, Slovak Republic

This study examined the antiproliferative effects of β -escin (E) in cancer cells. The study showed that E inhibited cancer cells growth in a dose-dependent manner. The flow cytometric analysis revealed an escin-induced increase in the sub-G1 DNA content, which is considered to be a marker of apoptosis. Apoptosis was also confirmed by annexin V staining and DNA fragmentation assay. These effects were associated with increased generation of reactive oxygen species (ROS), caspase-3 activation and decreased mitochondrial membrane potential (MMP). Moreover, escin decreased mitochondrial protein content and mitochondrial fluorescence intensity as well as caused depletion of glutathione (GSH). However, activity of glutathione peroxidase (GPx) and glutathione reductase (GR) was not significantly changed in escin-treated cells. In conclusion, our results demonstrated that E has apoptotic effects in human cancer cells through the mechanisms involving mitochondrial perturbation. Although the exact mechanism needs to be investigated further, it can be concluded that E may be a useful candidate agent for cancer treatment.

Key words: escin, apoptosis, mitochondria, fluorescence fingerprint

Received: 22 March, 2015; **revised:** 05 November, 2015; **accepted:** 24 November, 2015; **available on-line:** 27 January, 2016

INTRODUCTION

Horse chestnut (*Aesculus hippocastanum*) is one of the oldest and widely used medicinal plant since ancient times. For example, the extracts from the horse chestnut seeds have been traditionally used in China as a carminative, stomachic, and anti-inflammatory agent in treating varicosis, in general, and hemorrhoids, in particular (Sirtori, 2001; Pittler & Ernst, 2012; Suter *et al.*, 2006; Wang *et al.*, 2013). The primary active constituent found in horse chestnut seed extract is a triterpene saponin β -escin (Sirtori, 2001). A number of other compounds such as bioflavonoids (quercetin, kaemferol and their diglycosyl derivatives), and coumarins (aesculin and fraxin) have been isolated from the chestnut seeds (Sirtori, 2001; Bombardelli & Morazzoni, 1996; Patlolla *et al.*, 2006). Escin was found to be effective as anti-inflammatory, antiviral, antiallergic, antioxidant and vasorelaxant agent (Küçük Kurt *et al.*, 2010; Lindner *et al.*, 2010; Čalić-Dragosavac *et al.*, 2011). Moreover, ability of β -escin to suppress growth of cancer cells has also been documented by Guo *et al.* (2003) found that β -escin can inhibit the growth of various human and mice tumor cell lines and the tumors developed after their transplantation. Later, Niu and co-workers demonstrated that β -escin is a po-

tent natural inhibitor of cell proliferation and inducer of apoptosis in K 562 chronic myeloid leukemia cells (Niu *et al.*, 2008). Escin was also found to exhibit significant antitumor effects in human hepatocellular carcinoma both *in vitro* and *in vivo* (Zhou *et al.*, 2009). Recently, Ji and coworkers (2011) found that the antiproliferative effect of escin may be related to inhibition of the JAK/STAT signaling pathway. Furthermore, other signaling pathways may also be involved in anticancer effect of escin. It is accepted that nuclear factor- κ B (NF- κ B) signalling pathway plays an important role in physiological as well as pathological processes, including tumorigenesis (Shishodia & Aggarwal, 2004). In the study of Harikumar *et al.* (2010), Wang *et al.* (2012) and Rimmon *et al.* (2013) escin was found to downregulate NF- κ B signaling pathway with subsequent induction of apoptosis or sensitization of cancer cells to standard chemotherapy.

Recently, we also demonstrated that extract of horse chestnut (HCE) possesses antiproliferative and antiangiogenic properties. We found that HCE inhibited growth and colony formation, and induced apoptosis in cancer cells. Moreover, HCE inhibited migration of endothelial cells as well as decreased the secretion of matrix metalloproteinase and vascular endothelial growth factor (Mojžišová *et al.*, 2013). Because E is the main active component of horse chestnut, the aim of this study was to evaluate possible mechanism of its antiproliferative effect.

MATERIALS AND METHODS

Chemicals. Pure β -escin was a gift from CALENDULA a. s. (Nová Ľubovňa, Slovak Republic). Cycle TEST™ PLUS DNA Reagent Kit and propidium iodide were purchased from Becton Dickinson Biosciences (BDB, San Jose, CA, USA). 3-(4,5-Dimethylthiazol-2-yl)-2,5-diphenyltetrazolium bromide (MTT) was from Sigma-Aldrich (St. Louis, MO, USA). Dipotassium hydrogen phosphate (K_2HPO_4), ethylenediamine tetraacetic acid (EDTA), magnesium chloride ($MgCl_2$), potassium chloride (KCl), potassium dihydrogen phosphate (KH_2PO_4), sodium succinate ($NaOOCCH_2CH_2COONa \times 6H_2O$), TRIS HCl, sucrose and dimethyl sulfoxide

✉ e-mail: gabriela.mojzisova@upjs.sk

Abbreviations: ATCC, American Type Culture Collection; DHR-123, dihydrorhodamine-123; DMSO, dimethyl sulfoxide; E, β -escin; FCM, flow cytometry; GPx, glutathione peroxidase; GR, glutathione reductase; GSH, glutathione; CHCE, horse chestnut extract; MMP, mitochondrial membrane potential; MTT, 3-(4,5-dimethylthiazol-2-yl)-2,5-diphenyltetrazolium bromide; ROS, reactive oxygen species; SDS, sodium dodecylsulfate; SOD, superoxide dismutase

(DMSO), glutathione reductase (GR), glutathione peroxidase (GPx) assay kit and sodium dodecylsulfate (SDS) were obtained from Sigma–Aldrich Chemie (Steinheim, Germany). Superoxide dismutase (SOD) assay Kit–WST was purchased from Fluka (Japan). RPMI 1640 medium was from PAA Laboratories (Pasching, Austria). High glucose Dulbecco's Modified Eagle Medium, fetal calf serum, penicillin, and streptomycin were obtained from Invitrogen (Carlsbad, CA USA). Proteinase K and RNase were purchased from Amresco (USA).

Cell lines and culture. The following human cancer cell lines were used for this study: Jurkat (human acute T-lymphoblastic leukaemia), CEM (acute T-lymphoblastic leukaemia), HeLa (cervical carcinoma cells), and MCF-7 (breast cancer cells). All cell lines used were purchased from American Type Culture Collection (ATCC). Jurkat, CEM and HeLa cells were cultured in RPMI 1640 medium. MCF-7 cells were cultured in growth medium consisting of high glucose Dulbecco's Modified Eagle Medium. Both media were supplemented with Glutamax and 10% fetal calf serum, penicillin (100 IU/mL), and streptomycin (100 µg/mL). Cells were kept at 37°C in a humidified atmosphere with 5% CO₂. Cell viability, estimated by trypan blue exclusion, was greater than 95% before each experiment.

Growth inhibition assay. The antiproliferative effect of E was studied by MTT assay (Mosman, 1983). The method is based on the conversion of tetrazolium dye MTT 3-(4,5-dimethylthiazol-2-yl)-2,5-diphenyltetrazolium bromide inside the cells to insoluble formazan. The stock solution of E was prepared in DMSO and diluted to a different concentration. The final concentration of DMSO in culture medium was 0.2%.

Briefly, cells were seeded on 96-well plates (Sarstedt, Nümbrecht, Germany) at density of 8×10^3 cells/well in 80 µL of the medium. After 24 h of adhesion, 20 µL aliquots of E (7.8–500.0 µg/mL) were added. After 72 h of culturing, 10 µL of the MTT solution were added to each well and the cells were incubated for another 4 h. Then, the formazan crystals were dissolved with 100 µL of 10% SDS. The absorbance was measured at 540 nm using the automated uQuant™ Universal Microplate Spectrophotometer (Biotek, Winooski, VT, USA). The absorbance of the control wells was taken as 100% and the results were expressed as the percentage of the control (untreated cells).

xCELLigence cell analysis system. xCELLigence system is a unique, impedance-based system for cell-based assays, allowing for label-free and real-time monitoring of cellular processes such as cell growth, proliferation, cytotoxicity, adhesion, morphological dynamics and modulation of barrier function. It measures impedance changes in a meshwork of interdigitated gold microelectrodes located at the well bottom (E-plate) or at the bottom side of a microporous membrane (CIM16-plate). These changes are caused by the gradual increase of electrode surface occupation by (proliferated/ migrated/ invaded) cells during the course of time and thus can provide an index of cell viability, migration and invasion. This method of quantitation is directly proportional to cellular morphology, spreading, ruffling and adhesion quality as well as cell number (Ke *et al.*, 2011).

The xCELLigence RTCA system was initialized, as per manufacturer's instructions, prior to commencement of the experiment by filling all 16 wells of the E-plate (ACEA Biosciences) with the growth medium (100 µL), and equilibrated at room temperature for 30 min. The plate was placed into the single plate (SP) station cradle (housed in a humidified incubator at 37°C with 5% CO₂

atmosphere) to establish the background reading. Then, HeLa cells were seeded in E-plates at density of 2×10^5 cells per well. After 24 h, escin was added at concentrations of 31.2 and 62.5 µg/mL and cells were allowed to grow for additional 72 h under label-free conditions. The electrical impedance was measured by the RTCA-integrated software of the xCELLigence system (ACEA Biosciences) as a dimensionless parameter termed CI.

Colony formation analysis. For colony formation assay, HeLa cells were seeded in six-well plates at density of 1 000 cells per well and allowed to adhere for 10 h before treatment. RPMI 1640 medium containing various concentrations of E was added to the cells and the plates were incubated for 14 days. The cells were then fixed in buffered formalin (pH 7.2), stained with 0.01% crystal violet and washed to remove excessive dye. Quantitative changes in clonogenicity were determined by extracting the colonies with 10% acetic acid for 60 minutes and measuring the absorbance of the extracted dye at 540 nm. Cell survival at each drug concentration was expressed as a percentage of survival in comparison to the controls (untreated cells).

Cell cycle analysis. Cell cycle distribution in cells treated with the tested agents was analysed by propidium iodide (PI) DNA staining. Briefly, 5×10^5 Jurkat cells were treated with tested compounds for 24, 48 and 72 h. After treatment, cells were harvested, washed twice in PBS and fixed overnight in 70% ethanol at 4°C. Then, cells were washed with PBS, incubated for 1 h with 1 mg/mL RNase and 10 µg/mL PI at room temperature in the dark. After staining, samples were immediately analysed in FACS Canto flow cytometer using FACS Diva software (Becton Dickinson, USA). Ten thousand cells were acquired per sample. Data were analysed using Win MDI software and represented in the form of histograms. Percentages of cells corresponding to G₀/G₁, S and G₂/M phases of the cell cycle were calculated. The cells with DNA content lower than that of G₁-phase cells (hypoploid population) were considered to be apoptotic (sub-G₁).

Annexin V-FITC labelling. The plasma membrane changes characteristic of apoptosis were analysed by double staining with Annexin V-FITC and PI according to the manufacturer's instructions. Jurkat cells (1×10^5) were harvested 24, 48 and 72 h after treatment and stained with Annexin V-FITC (BD Biosciences Pharmingen, San Diego, CA, USA) in binding buffer for 15 min, washed, stained with PI for 5 min and thereafter analysed using BD FACS Calibur flow cytometer. Three populations of the cells were observed: viable cells: Annexin V-FITC negative and PI negative; apoptotic cells: Annexin V-FITC positive and PI negative; late apoptotic/necrotic cells: Annexin V-FITC positive and PI positive or Annexin V-FITC negative and PI positive.

DNA fragmentation assay. Treated and untreated Jurkat cells (for 24, 48 and 72 h; 1×10^6) were washed twice with phosphate-buffered saline w/o calcium and magnesium. Cells were lysed in a lysis buffer containing 10 mmol/L tris (hydroxymethyl)aminomethane, 10 mmol/L EDTA, 0.5% Triton X-100. Proteinase K (1 mg/mL) was added and cells were incubated at 37°C for 1 h. Subsequently, 10 min incubation at 70°C was performed. Then, RNase (200 mg/mL) was added and cells were incubated for another 1 h at 37°C. Samples were transferred to 2% agarose gel and run at 40 V for 3 h. DNA fragments were visualized with UV illuminator after ethidium bromide staining.

Measurement of ROS. The intracellular production of ROS was detected with FCM analysis using dihy-

diorhodamine-123 (DHR-123, Fluka, Buchs, Switzerland), which reacts with intracellular hydrogen peroxide. Jurkat cells treated with an appropriate agent were harvested, washed twice with PBS, and resuspended in PBS. DHR-123 was added at a final concentration of 0.2 μ M. The samples were then incubated for 15 min in the dark and placed on ice after the incubation. Fluorescence was detected with 530/30 (FL-1) optical filter. Forward and side scatters were used to gate the viable populations of cells.

Detection of MMP. The changes in MMP were analysed with FCM using tetramethylrhodamine ethyl ester perchlorate (TMRE, Molecular Probes, Eugene, OR, USA). Jurkat cells were washed with PBS, resuspended in 0.1 μ M of TMRE in PBS, and incubated for 30 min at room temperature in the dark. The cells were then washed twice with PBS, resuspended in 500 μ L of the total volume, and analysed (1×10^4 cells per sample). Fluorescence was detected with 585/42 (FL-2) optical filter.

Detection of active caspase 3. The changes in caspase 3 activation were analysed with FCM using BD Pharmingen Active Caspase-3 PE MAb Apoptosis kit (BD Bioscience, San Diego, CA, USA). Jurkat cells were prepared according to manufacturer's guidelines, stained with PE conjugated antibody and incubated for 30 min at room temperature in the dark. The cells were then washed twice with PBS, resuspended in 500 μ L of the total volume and analysed (1×10^4 cells per sample). Fluorescence was detected with 585/42 (FL-2) optical filter.

Mitochondria isolation, determination of proteins and enzymes activities. Mitochondria were isolated from Jurkat cells according to the method of Mela & Seitz (1979). Cells were incubated for 72 hours with E (31.2 μ g/mL).

The medium for mitochondria isolation pH=7.2 consisted (in mol/L) of sucrose 0.25, EDTA 0.002, TRIS HCl 0.010. The content of proteins in isolated mitochondria was estimated with the method of Bradford (1976).

Kinetic methods for estimating the activities of glutathione peroxidase (GPx, E.C. 1.11.1.9), glutathione reductase (GR, E.C.1.6.4.2) and superoxide dismutase (SOD, E.C. 1.15.1.1) were applied according to the manufacturer's instructions.

The reduced glutathione (GSH) level was determined by the method of Floreani *et al.* (1997) using Ellman's reagent ($R^2=0.9923$). Camspec M501 Single Beam Scanning UV/VIS spectrophotometer (Spectronic Camspec Ltd., Leeds, UK) was used for the enzyme assays.

Fluorescence spectra measurements. The fluorescence spectra were analysed with Perkin Elmer Model LS 55 luminescence spectrometer using 1 cm pathlength quartz cuvettes at ambient temperature. The wavelength scan speed of both monochromators was 1200 nm/min. The setting for instrument's excitation slit was 10 nm and the one for the emission slit was 15 nm.

Immediately before use, the isolated mitochondria have been diluted 1:100 in respiration media containing 1 mM sodium succinate. The mitochondrial characteristic pattern in respiration medium was investigated by synchronous fluorescence fingerprint (SFF).

The synchronous spectra have been measured at the constant setting of difference between emission and excitation monochromators $\Delta\lambda=10-200$. The setting for excitation wavelengths was 200-400 nm. The contour lines of 3-D spectra were constituted from 20 (number of scans) simple spectral records of mitochondria and

placed in space with increment (distance) of 10. Data processing was managed by the FL Winlab (Perkin-Elmer) software package.

Statistical analysis. Statistical data was expressed as mean \pm standard deviation (S.D.). Student's *t*-test and analysis of variance were employed to determine statistical significance. Values of $p < 0.05$, $p < 0.01$ and $p < 0.001$ were considered to be statistically significant.

RESULTS

Effect of escin on cell proliferation

In this study we used a microculture assay based on metabolic reduction of MTT to evaluate the antiproliferative effect of E on four cancer cell lines. Survival of CEM, HeLa, Jurkat as well as MCF-7 cells exposed to various E concentrations is shown in Fig 1a. At the higher concentrations of E (62.5-500.0 μ g/mL), cell viability was suppressed almost completely. At the concentration of 31.25 μ g/mL, E caused 44.7%, 42.7%, 86.4%, and 41.7% reduction in cell survival ($p < 0.001$; $p < 0.01$). Moreover, E at the concentration of 15.6 μ g/mL significantly decreased Jurkat and MCF cells survival ($p < 0.05$; $p < 0.01$). IC_{50} ranged from 21.2 to 42.9 μ g/mL (Fig. 1b).

The antiproliferative effect of compound β -escin on HeLa cells was also evaluated by xCELLigence system. As shown in Fig. 2 cell index of HeLa cells decreased significantly after treatment with E in a concentration-dependent manner.

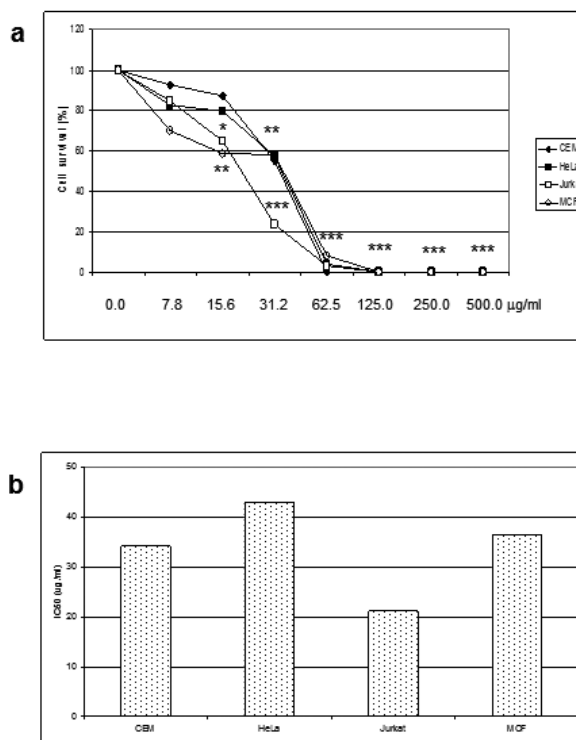


Figure 1. Survival of HeLa, CEM, Jurkat and MCF cancer cells after 72 h of cultivation with β -escin (a). IC_{50} values (b; μ g/mL) of β -escin for HeLa, CEM, Jurkat and MCF cancer cells after 72 h of cultivation. The results are presented from five independent experiments. * $p < 0.05$, ** $p < 0.01$, *** $p < 0.001$ vs. control (untreated cells).

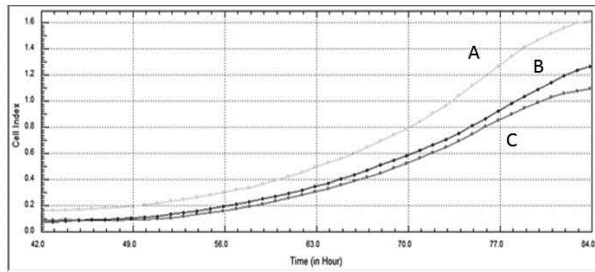


Figure 2. Real-time monitoring of HeLa cells proliferation after incubation with β -escin using the xCELLigence system. (A) untreated HeLa cells; (B) escin-treated cells (31.2 $\mu\text{g/ml}$); (C) escin-treated cells (62.5 $\mu\text{g/ml}$). The picture shown is representative of three independent experiments.

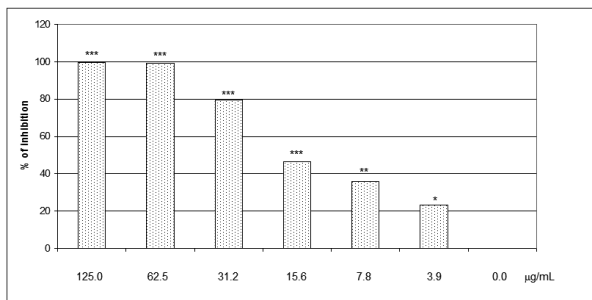


Figure 3. Effect of β -escin on colony formation by HeLa cells. The results are presented from five independent experiments. * $p < 0.05$, ** $p < 0.01$, *** $p < 0.001$ vs. control (untreated cells).

Escin inhibits colony formation

To analyze further the antiproliferative effects of E on anchorage-independent cell growth, we tested the ability of this compound to inhibit colony formation in a clonogenic assay. In accordance with MTT assay, E inhibited the clonogenic survival of HeLa cells during colony formation assay in dose dependent manner (Fig. 3) ($p < 0.001$; $p < 0.01$; $p < 0.05$).

Effect of escin on cell cycle

To examine the potential mechanism through which E suppresses cell proliferation, we examined the cell cycle profiles of Jurkat cells treated with E (31.2 $\mu\text{g/ml}$).

The results of the cell cycle analysis revealed that E significantly increased the percentage of cells with sub- G_1 DNA content. As shown in Table 1, the cell population undergoing apoptosis (the sub- G_1 content) increased to 80.1% after 72 hours of incubation compared to 3.3% in untreated cells ($p < 0.001$). This ef-

Table 1. Flow cytometric analysis of cell cycle distribution in Jurkat cells treated with β -escin (31.2 $\mu\text{g/ml}$) (in %).

Treatment	Time	sub- G_1	G0/G1	S	G2/M
C		3.3 \pm 0.7	58.5 \pm 3.1	14.7 \pm 1.3	23.3 \pm 2.5
	24 h	39.7 \pm 2.8***	35.8 \pm 3.1	15.6 \pm 0.6	8.9 \pm 0.8
E	48 h	73.2 \pm 7.1***	15.4 \pm 2.8	9.2 \pm 1.1	2.2 \pm 1.3
	72 h	80.1 \pm 3.6***	12.5 \pm 2.3	6.2 \pm 2.0	1.2 \pm 2.0

E, β -escin; C, Control. The results are presented from five independent experiments. *** $p < 0.001$

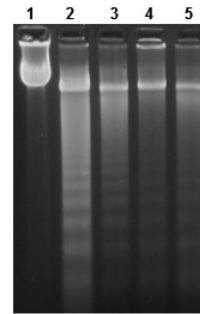


Figure 4. The effect of β -escin (E; 31.2 $\mu\text{g/ml}$) on the presence of DNA fragments in Jurkat cells incubated for 24, 48, 72 h. Control (lane 1), positive control (etoposide 50 $\mu\text{g/ml}$ for 72 h) (lane 2), 24 h (lane 3), 48 h (lane 4) and 72 h (lane 5) of incubation.

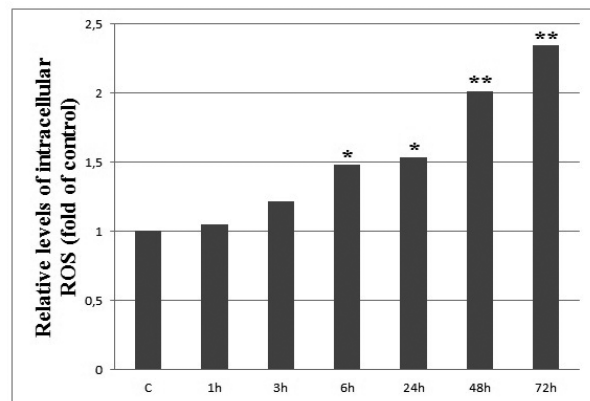


Figure 5. Measurement of ROS production in Jurkat cells treated with β -escin.

Cytosolic ROS were measured 1, 3, 6, 24, 48 and 72 h after treatment by quantifying the fluorescence intensity of activated DHR-123. The results (mean \pm S.D.) of three independent experiments are shown as multiples of the control group fluorescence. * $p < 0.05$, ** $p < 0.01$, vs. control (untreated cells)

fect was accompanied by a proportional decrease in the percentage of cells in G0/G1, S and G2/M phase.

Escin induces apoptotic cell death

It has been generally accepted that the increase of cells having sub- G_1 DNA content is a marker of apoptotic cell death. To clarify whether or not the escin-induced cell death involves apoptosis, flow cytometry analysis was employed. We found that β -escin significantly increased percentage of cells in early apoptosis in a time-dependent manner after 24, 48 and 72 h of treatment (10.44–31.88% vs. 3.52% in untreated cells). Simultaneously, percentage of annexin V/PI positive cells increased from 3.38% (control) to 28.15% (E-treated cells after 72 h of incubation). These experimental results demonstrate that E induced apoptosis in Jurkat cells (Table 2).

DNA fragmentation assay

Analysis of DNA fragmentation by agarose gel electrophoresis is one of the most widely used biochemical markers for cell death. The detection of internucleosomal DNA cleavage (DNA laddering) is considered to be an indicator of apoptosis (Nagata, 2000).

Table 2. Induction of apoptosis after β -escin treatment measured with Annexin V/PI staining.

Jurkat cells were treated with E (31.2 $\mu\text{g}/\text{mL}$) for 24, 48 and 72 h, stained with fluoresceinated Annexin V and propidium iodide (PI), and analysed using flow cytometry.

Treatment	Time	An ⁻ /PI ⁻	An ⁺ /PI ⁻	An ⁺ /PI ⁺
C		93.1 \pm 0.42	3.52 \pm 0.70	3.38 \pm 0.59
	24 h	80.24 \pm 2.11*	10.44 \pm 1.13*	9.32 \pm 0.93
E	48 h	59.91 \pm 2.20**	22.88 \pm 2.19**	17.21 \pm 1.84*
	72 h	39.97 \pm 3.35***	31.88 \pm 2.46***	28.15 \pm 2.19**

E, β -escin; C, Control. An⁻/PI⁻, viable cells; An⁺/PI⁻, early apoptotic cells; An⁺/PI⁺, late apoptotic/necrotic cells. The results are presented from five independent experiments. * $p < 0.05$; ** $p < 0.01$; *** $p < 0.001$

As shown in Fig. 4, treatment of Jurkat cells with E (31.2 $\mu\text{g}/\text{mL}$) resulted in the formation of definite fragments that were visible during the electrophoresis as the characteristic ladder pattern (for 24, 48 and 72 h).

Escin stimulates ROS production

Reactive oxygen species (ROS) have been documented to activate either extrinsic or intrinsic apoptotic pathway (Circu & Aw, 2010). Because the production of ROS can be associated with escin-induced apoptosis, we decided to verify whether escin was able to stimulate ROS generation with flow cytometry and using the fluorescent probe rhodamine 123.

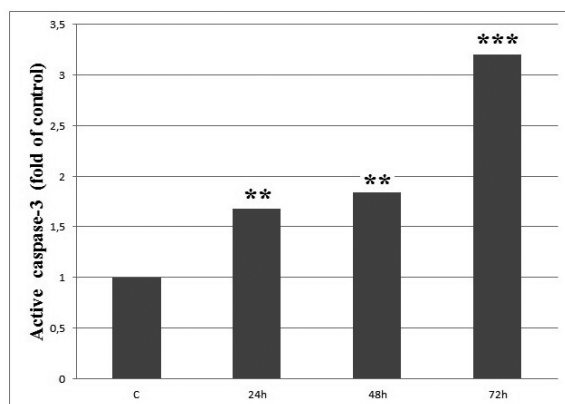
As shown in Fig. 5, E induced ROS increase in a time dependent manner in Jurkat cells. There was a significant increase in the ROS levels starting from 6 h and continuing up to 72 h ($p < 0.05$ and $p < 0.01$, respectively).

Activation of caspase-3 by escin

Caspase-3 is a crucial mediator of programmed cell death. To confirm whether E-induced cell death is associated with the activation of caspase-3, we analysed its activity with flow cytometry. We observed time-dependent increase in caspase-3 activity in E-treated Jurkat cells (Fig. 6).

Escin decreases mitochondrial membrane potential

There is accumulating evidence suggesting that loss of MMP can be associated with apoptosis. To evaluate mi-

**Figure 6. Effect of β -escin treatment on caspase-3 activation.**

Caspase-3 activation was measured 24, 48 and 72 h after treatment by quantifying the fluorescence intensity. * $p < 0.05$, ** $p < 0.01$, *** $p < 0.001$ vs. control (untreated cells).

tochondrial membrane integrity, a highly specific probe for detection of changes in MMP (cationic dye TMRE) was used. Treatment of Jurkat cells with E (31.2 $\mu\text{g}/\text{mL}$) led to dissipation of MMP in a time-dependent manner (Fig. 7).

Effect of escin on mitochondrial protein content

Pre-treatment of Jurkat cells with E significantly decreased protein content in mitochondria in comparison to untreated cells (Table 3) ($p < 0.01$).

Effect on mitochondrial fluorescence spectra

The synchronous fluorescence fingerprint (SFF) of mitochondrial autofluorescence and horizontal cut of SFF at $\Delta\lambda = 50$ nm are methods which in a simplistic form describe the fluorophores of outer mitochondrial membrane (Fig. 8A, 8B). Topographic map of SFF shows a specific pattern of spatial distribution of fluorescence for a given mitochondrial suspension after isolation. This mixture is the final result of total fluorescence of all fluorophores which are present in the mitochondria and reflects the quality of mitochondria.

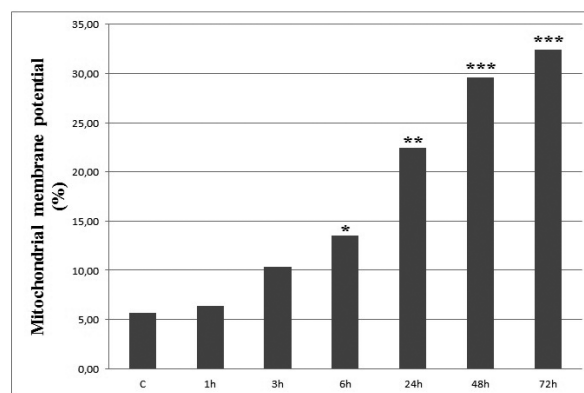
It is considered as a characteristic "fingerprint" with maximum of fluorescence at $\lambda = 70/283$ nm for control mitochondria (Table 3, Fig. 8A). The maximum of fluorescence was markedly changed in mitochondria from E-treated cells ($\lambda = 30/276$) (Table 3, Fig. 8A).

Horizontal cut of SFF at selected $\Delta\lambda = 50$ nm (Fig. 8B) of control and experimental mitochondria revealed two main characteristic fluorescence zones of mitochondrial mixture. The first zone (zone 1), a large peak of fluorescence located at 280/340 nm (excitation/emission) is consistent with protein fluorescence and most of the emission is due to excitation of tryptophan residues. The second zone (zone 2), a smaller peak at 350/400 nm is consistent mainly with NADH fluorescence (Kirkpatrick *et al.*, 2005; Tomečková *et al.*, 2011).

Our results showed that E influenced fluorescence of mitochondria isolated from Jurkat cells. We found decrease of fluorescence signal in the zone 1 as well as in the zone 2 in comparison with control mitochondria (Table 3, Fig. 9).

Enzyme activities and GSH content

Dismutation of superoxide radicals results in the formation of hydrogen peroxides by superoxide dismutase

**Figure 7. MMP changes in Jurkat cells treated with β -escin were analysed 1, 3, 6, 24, 48 and 72 h after treatment.**

* $p < 0.05$, ** $p < 0.01$, *** $p < 0.001$ vs. control (untreated cells).

Table 3. Protein content of mitochondria isolated from Jurkat cells and fluorescence centres evaluated from synchronous fluorescence fingerprint of mitochondria.

Treatment ($\mu\text{g/mL}$)	Protein content (mg/mL)	Centre of fluorescence $\Delta\lambda / \lambda_{\text{ex}}$ (nm)	Fluorescence F
Control	0.52	$\Delta 70 / 283$	566
E (31.2)	0.079**	$\Delta 30 / 276$	512

E, β -escin; $\Delta\lambda$, difference between emission and excitation wavelength; λ_{ex} , excitation wavelength; $\Delta\lambda / \lambda_{\text{ex}}$, point at synchronous fluorescence fingerprint with the maximum fluorescence intensity. ** $p < 0.01$

(SOD). SOD activity in mitochondria from E-treated cells significantly increased in comparison with control ($p < 0.001$, Fig. 10A). Increase in SOD activity was associated with increased activity of GPx and GR. However, changes in metabolic activity of GPx and GR did not reach statistical significance (Fig. 10B, 10C).

GSH plays an important role in protection against oxidative stress-induced injury and intracellular GSH depletion results in apoptosis. We therefore analysed changes in the mitochondrial GSH level in E-treated Jurkat cells. As shown in Fig. 10D, a significant decrease in GSH content was observed in E-treated cells as compared to untreated cells ($p < 0.001$).

DISCUSSION

Cancer is one of the most important health problems in the world. In spite of the progress in cancer therapy, it is still necessary to develop new therapeutic strategies. Natural compounds, as highlighted also in this study, are becoming an important research area for novel and bioactive molecules for drug discovery (Vidinský *et al.*, 2012; Bak *et al.*, 2013; Tepe *et al.*, 2013).

In the present study we aimed to analyze the effect of β -escin on the viability and proliferation of cancer cells. First, we evaluated the antiproliferative effect of this compound by MTT assay and impedance-based real-time cellular assay. In our *in vitro* studies, the treatment of cancer cells with E inhibited the growth of cells in a dose-dependent manner. Consistently with these results, it also suppressed clonogenic cell growth of HeLa cells and caused a significant decrease of cell viability at the concentration of $3.9 \mu\text{g/mL}$. However, the exact mechanisms by which β -escin exerts its growth-inhibitory effect in cancer cells remain unclear.

One of the hallmarks of cancer is the ability of cancer cells to avoid apoptosis (Hanahan & Weinberg, 2011). Therefore, the apoptotic pathways are an interesting target of cancer treatment and many of the anticancer agents in current use have been shown to induce apoptosis in cancer cells. In an attempt to determine the mechanism responsible for the antiproliferative effect of the compound tested, we assessed apoptosis using DNA content analysis, annexin V/PI staining and DNA fragmentation assay. In our study we observed that the decrease in cell viability resulting from E treatment was associated with a reduction in the proportion of Jurkat cells in the S, G₀/G₁ and G₂/M phases with concomitant increase in the fraction of cells with sub-G₁ DNA content which is considered to be a marker of apoptotic cell death. In comparison with untreated cells, in E-treated cells the number of cells with sub-G₁ DNA content was increased 12-, 22.2- and 24.3-fold after 24, 48 and 72 hours of treatment, respectively. Increase in the proportion of cells with sub-G₁ DNA content after exposure of Jurkat cells to E was also documented by Zhang *et al.*, 2011. To confirm whether E could induce

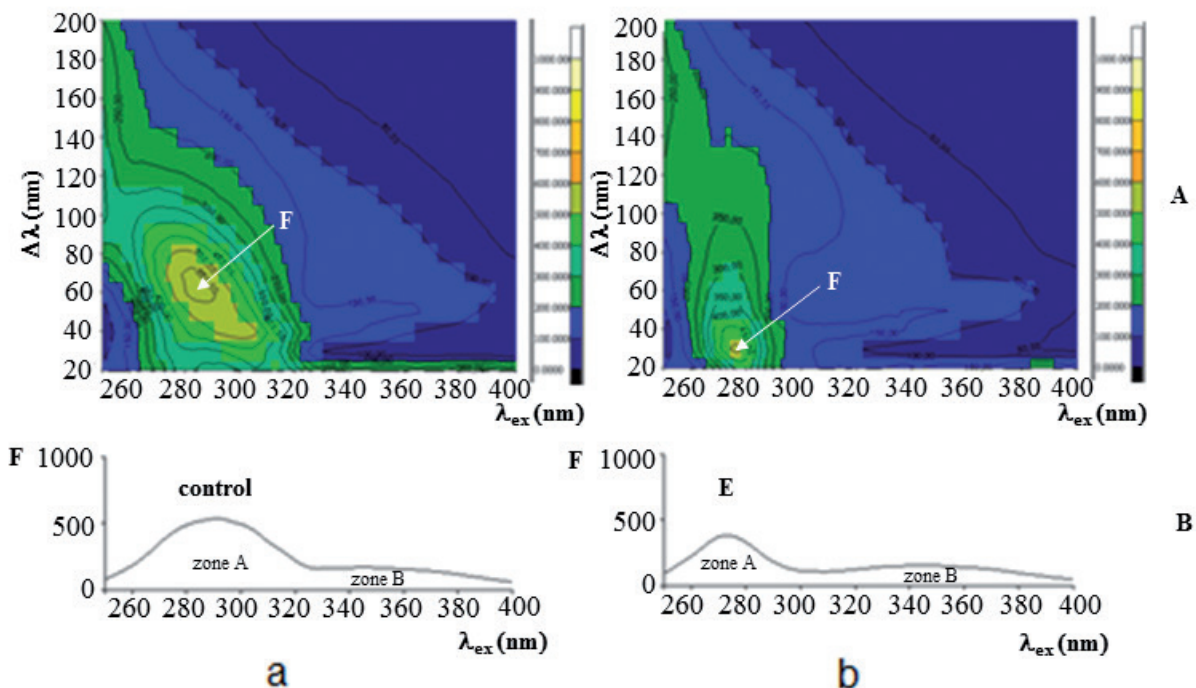


Figure 8. The topographic maps of synchronous fluorescence fingerprint (A) and horizontal cut of synchronous fluorescence fingerprint at $\Delta\lambda = 50 \text{ nm}$ (B) of control and experimental mitochondria isolated from Jurkat cells treated with β -escin (E; $31.2 \mu\text{g/mL}$). The comparison of topographic maps of synchronous fluorescence fingerprints (SFF) of control (untreated cells) mitochondria (a) ($\lambda = \Delta 70/283 \text{ nm}$, $F = 566$) and experimental mitochondria isolated from E-treated cells (b) ($\lambda = \Delta 30/276 \text{ nm}$, $F = 512$). λ_{ex} , excitation wavelength; $\Delta\lambda$, difference between emission and excitation wavelength; F, fluorescence

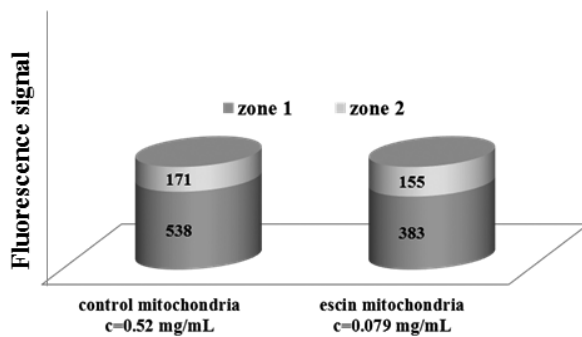


Figure 9. Comparison of the maximum fluorescence signal of the first and the second fluorescence zones of synchronous spectra $\Delta\lambda=50$ nm of control mitochondria isolated from Jurkat cells and experimental mitochondria isolated from Jurkat cells treated with β -escin (31.2 $\mu\text{g}/\text{mL}$).

The first and the second zone show the maximal total fluorescence intensities of all fluorophores present in control and experimental mitochondria. The proteins and their interaction with escin are shown in the first zone of fluorescence which is strongly affected by light scattering (should be taken into evaluation). The interaction of mitochondrial coenzyme $\text{NADH}+\text{H}^+$ with β -escin was studied in the second zone of fluorescence as marker of the presence of oxygen and respiration metabolism in mitochondria.

apoptosis in Jurkat cell line, we performed annexin V/PI staining, which detects both the early stage of apoptosis as well as the late stage of apoptosis/necrosis. Our results showed time-dependent decrease of vital cells number (An^-/PI^-) and a significant increase in annexin V positive cells (An^+/PI^- or An^+/PI^+). The presence of apoptosis induced by E was further evidenced by nuclear DNA fragmentation which is a classical feature of apoptotic cell death. Our experimental results demonstrated that E induces apoptosis of cancer cells. These findings also supported caspase-3 activation observed in E-treated cells that could be one of the crucial steps to execution of apoptotic features. Pro-apoptotic effect of

escin in different cancer cell lines has also been documented by other authors (Niu *et al.*, 2008; Çiftçi *et al.*, 2015; Güney *et al.*, 2013).

It is well known that mitochondria play essential roles in the cellular metabolism (Nemoto *et al.*, 2000). Mitochondria were also shown to be crucial for the regulation of intracellular Ca^{2+} homeostasis, redox signalling, and regulation of cell proliferation. In addition to their role in cellular energy metabolism, mitochondria are now recognised as central players in cell death (Olszewska & Szweczyk, 2013). Furthermore, it is well known that changes in the structure of mitochondrial membrane may lead to the induction of apoptosis (Gogvadze & Orrenius, 2006; Parsons & Green, 2010) associated with changes in MMP, intracellular ROS production and caspase activation (Lemasters 1999; Wu *et al.*, 2014). It was also stated that loss of MMP may increase permeability of the mitochondrial membrane with subsequent leakage of apoptogenic molecules from intermembrane space into the cytoplasm (Ly *et al.*, 2003). Hence, in our study, assessment of ROS species, mitochondrial function and activity of antioxidant system were carried out.

In our work, MMP was measured in order to examine whether apoptosis was accompanied by the loss of mitochondrial membrane potential. We found significant decrease of MMP in cancer cells 6 h after E treatment. Our results indicate that decrease of MMP may play a role in E-induced cell death. Moreover, according to our best knowledge, the effect of β -escin on MMP has not been documented previously.

Furthermore, mitochondria are also important source of ROS, which are produced there in a consequence of aerobic respiration and oxidative phosphorylation (Książkowska-Łakoma *et al.*, 2014). Under physiological conditions ROS are involved in specific functions, such as signalling and protein regulation (Okon & Zhou, 2015). On the other hand, ROS can oxidize proteins and induce lipid peroxidation, compromising the barrier properties of biological membranes (Gogvadze & Orrenius, 2006). An increase in ROS production can

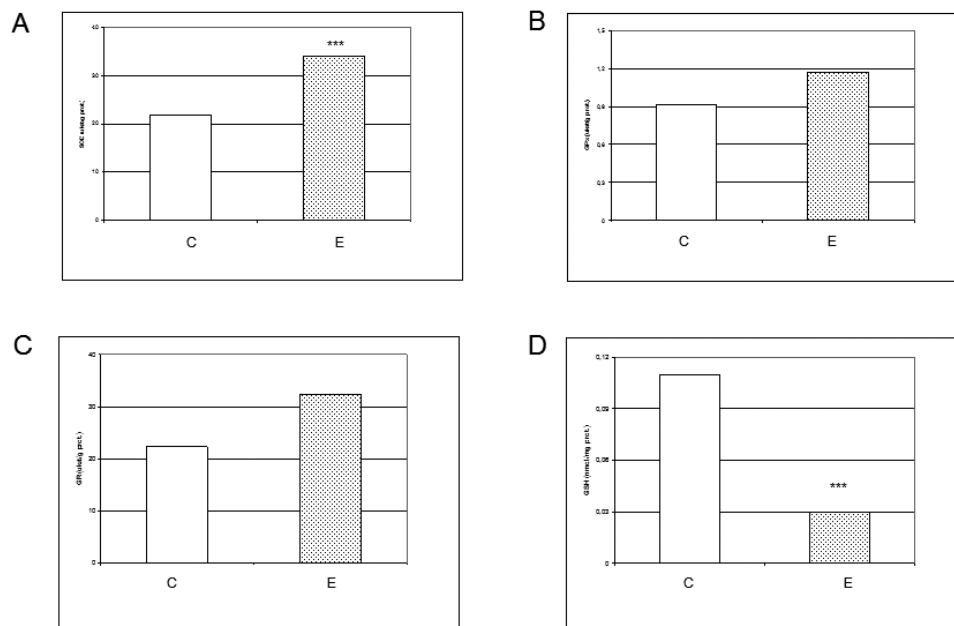


Figure 10. Effect of β -escin (E; 31.2 $\mu\text{g}/\text{mL}$) on the activity of superoxide dismutase (A; SOD), glutathione peroxidase (B; GPx), glutathione reductase (C; GR) and reduced glutathione (D; GSH) content in mitochondria.

Activities of all enzymes are expressed in $\mu\text{kat}/\text{g}$ of protein. GSH content is expressed in nmol/mg of protein. *** $p < 0.001$ vs. control (untreated cells).

result in the impairment of the mitochondrial function that triggers the apoptosis pathway (Fleury *et al.*, 2002). To investigate if the mitochondrial dysfunction found in E-treated Jurkat cells is initiated by ROS production, we measured ROS levels using the cell-permeable dye DHR-123. The result showed that E causes a rapid increase of intracellular ROS levels in Jurkat cells after 6 h of incubation. Other authors have also reported ability of E to generate ROS either in malignant (Shen *et al.*, 2011) or non-malignant cells (Zhang *et al.*, 2010).

Because there is a close relation between increased levels of ROS and MMP disruption (Mates *et al.*, 2012), we suggest that E-induced cell apoptosis in Jurkat cells might be mitochondria dependent.

Moreover, in the present study we also demonstrated the changes of outer mitochondrial membrane in E-treated cells. As it was mentioned above, fluorescence at zone 1 (280/340 nm; excitation/emission) is consistent with protein/tryptophan-related fluorescence. We found that E decreased tryptophan-related signal which is in correlation with decreased protein content of mitochondria isolated from E-treated cells. Similar decrease in tryptophan fluorescence related to protein content was also documented by Kirkpatrick and co-workers (2005).

Furthermore, the NADH-related signal (zone 2) was strongly decreased by E treatment. Because NADH plays a role not only in a wide range of cellular reactions (e.g. energy metabolism, calcium homeostasis) (Cortassa *et al.*, 2003), but may act as a natural biomarker for mitochondrial dysfunction (Heikal, 2010), our results indicated that mitochondria may be the target structures for E. This hypothesis is supported by the work of the Poque and co-workers (2001), who found that a decrease in NADH fluorescence is associated with mitochondrial membrane disruption. Furthermore, the study of Petit and co-workers (2001) indicated a close temporal relationship between decreased NADH fluorescence and the dissipation of the MMP. The similar decrease in the NADH fluorescence accompanied by a marked decrease of MMP and elevated intracellular ROS levels was also observed by Lemar *et al.*, (2007).

As it was mentioned previously, ROS are mediators involved in different physiological as well as pathological processes. To prevent tissue injury, ROS are eliminated either by enzymatic (e.g. SOD, CAT, GPx) or non-enzymatic (e.g. glutathione) protective mechanisms.

In the present study a significant increase in SOD activity and mild increase in GPx as well as GR activity was observed. Because increased activity of antioxidant enzymes may be an adaptive cellular response to increased oxidative stress (Kale *et al.*, 1999; Devi *et al.*, 2000), we suggest the same mechanism is present also in E-treated cells.

Furthermore, some anticancer agents have demonstrated that GSH depletion can increase ROS generation and subsequently induces apoptosis in different cancer cells (Khan *et al.*, 2012; Ong *et al.*, 2008). To understand whether GSH is related to the β -escin-induced increase in ROS levels in cancer cells, changes in GSH levels were assessed. We found significant decrease in GSH in cells exposed to E. Because GSH is the most abundant intracellular thiol and the GSH-dependent antioxidant system plays the central role in cellular protection against oxidant injury (Armstrong *et al.*, 2002), depletion of mitochondrial GSH increases susceptibility to oxidant injury (Marí *et al.*, 2013). These results suggest that the oxidative stress plays an important role in the antiproliferative effect of escin on Jurkat cells.

In conclusion, our results showed that E exerts apoptotic effects on human cancer cells through the mechanism involving ROS generation, loss of mitochondrial GSH content, decrease of MMP and caspase-3 activation. Changes of mitochondrial autofluorescence also indicate the mitochondrial dysfunction. Although the exact mechanisms need to be investigated further, the growth inhibitory properties of E on cancer cell proliferation indicated the potential use of this compound as a chemotherapeutic agent for the treatment of some carcinomas.

Acknowledgements

This work was supported by the Agency of the Slovak Ministry of Education for the Structural Funds of the EU, under project ITMS: 26220220104 (15%), ITMS: 26220120058 (15%) and ITMS: 26220220152 (15%). This study was also supported (50%) by the project Medicínsky univerzitný park v Košiciach (MediPark, Košice) ITMS:26220220185 (95 %) supported by Operational Programme Research and Development (OP VaV-2012/2.2/08-RO) (Contract No. OPVaV/12/2013).

REFERENCES

- Armstrong JS, Steinauer KK, Hornung B, Irish JM, Lecane P, Birrell GW, Peehl DM, Knox SJ (2002) Role of glutathione depletion and reactive oxygen species generation in apoptotic signaling in a human B lymphoma cell line. *Cell Death Differ* **9**: 252–263. doi: 10.1038/sj/cdd/4400959.
- Bak Y, Ham S, Baatartsogt O, Jung SH, Choi KD, Han TY, Han IY, Yoon DY (2013) A1E inhibits proliferation and induces apoptosis in NCI-H460 lung cancer cells *via* extrinsic and intrinsic pathways. *Mol Biol Rep* **40**: 4507–4519. doi: 10.1007/s11033-013-2544-0.
- Bombardelli E, Morazzoni P (1996) *Aesculus hippocastanum* L. *Fitoterapia* **67**: 483–511.
- Bradford MM (1976) A rapid and sensitive method for the quantitation of microgram quantities of protein utilizing the principle of protein-dye binding. *Anal Biochem* **72**: 248–254. doi:10.1016/0003-2697(76)90527-3.
- Čalić-Dragosavac D, Stević S, Zdravković-Korać S, Milojević J, Cingel A, Vinterhalter B (2011) Secondary metabolite of horse chestnut *in vitro* culture. *Adv Environ Biol* **5**: 267–270.
- Çiftçi GA, Işcan A, Kutlu M (2015) Escin reduces cell proliferation and induces apoptosis on glioma and lung adenocarcinoma cell lines. *Cytotechnology* **67**: 893–904. doi: 10.1007/s10616-015-9877-6.
- Circu ML, Aw TY (2010) Reactive oxygen species, cellular redox systems, and apoptosis. *Free Radic Biol Med* **48**: 749–762. doi: 10.1016/j.freeradbiomed.2009.12.022.
- Cortassa S, Aon MA, Marbán E, Winslow RL, O'Rourke B (2003) An integrated model of cardiac mitochondrial energy metabolism and calcium dynamics. *Biophys J* **84**: 2734–2755. doi:10.1016/S0006-3495(03)75079-6.
- Devi GS, Prasad MH, Saraswathi I, Raghu D, Rao DN, Reddy PP (2000) Free radicals antioxidant enzymes and lipid peroxidation in different types of leukemias. *Clin Chim Acta* **293**: 53–62. doi:10.1016/S0009-8981(99)00222-3.
- Fleury C, Mignotte B, Vayssières JL (2002) Mitochondrial reactive oxygen species in cell death signaling. *Biochimie* **84**: 131–141. doi:10.1016/S0300-9084(02)01369-X.
- Floreani M, Petrone M, Debetto P, Palatin P (1997) A comparison between different methods for the determination of reduced and oxidized glutathione in mammalian tissues. *Free Radic Res* **26**: 449–455. doi: 10.3109/10715769709084481.
- Gogvadze V, Orrenius S (2006) Mitochondrial regulation of apoptotic cell death. *Chem Biol Interact* **163**: 4–14. doi:10.1016/j.cbi.2006.04.010.
- Güney G, Kutlu HM, Işcan A (2013) The apoptotic effects of escin in the H-Ras transformed 5RP7 cell line. *Phytother Res* **27**: 900–905. doi: 10.1002/ptr.4804.
- Guo W, Bull Xu B, Yang XW, Liu Q, Cui JR (2003) The anticancer effect of β -escin sodium. *Chin Pharmacol* **19**: 351–352.
- Hanahan D, Weinberg RA (2011) Hallmarks of cancer: the next generation. *Cell* **144**: 646–674. doi: 10.1016/j.cell.2011.02.013.
- Harikumar KB, Sung B, Pandey MK, Guha S, Krishnan S, Aggarwal BB (2010) Escin, a pentacyclic triterpene, chemosensitizes human tumor cells through inhibition of nuclear factor-kappaB signaling pathway. *Mol Pharmacol* **77**: 818–827. doi: 10.1124/mol.109.062760.
- Heikal AA (2010) Intracellular coenzymes as natural biomarkers for metabolic activities and mitochondrial anomalies. *Biomark Med* **4**: 241–263. doi: 10.2217/bmm.10.1.

- Ji DB, Xu B, Liu JT, Ran FX, Cui JR (2011) β -Escin sodium inhibits inducible nitric oxide synthase expression via downregulation of the JAK/STAT pathway in A549 cells. *Mol Carcinog* **50**: 945–960. doi: 10.1002/mc.20762.
- Kale M, Rathore N, John S, Bhatnagar D (1999) Lipid peroxidative damage on pyrethroid exposure and alterations in antioxidant status in rat erythrocytes: a possible involvement of reactive oxygen species. *Toxicol Lett* **105**: 197–205. doi:10.1016/S0378-4274(98)00399-3.
- Ke N, Wang X, Xu X, Abbasi YA (2011) The xCELLigence system for real-time and label-free monitoring of cell viability. *Methods Mol Biol* **740**: 33–43. doi: 10.1007/978-1-61779-108-6_6.
- Khan M, Yi F, Rasul A, Li T, Wang N, Gao H, Gao R, Ma T (2012) Alantolactone induces apoptosis in glioblastoma cells via GSH depletion, ROS generation, and mitochondrial dysfunction. *IUBMB Life* **64**: 783–794. doi: 10.1002/iub.1068.
- Kirkpatrick ND, Zou C, Brewer MA, Brands WR, Drezek RA, Utzinger U (2005) Endogenous fluorescence spectroscopy of cell suspensions for chemopreventive drug monitoring. *Photochem Photobiol* **81**: 125–134. doi: 10.1111/j.1751-1097.2005.tb01531.x.
- Küçük Kurt I, Ince S, Keleş H, Akkol EK, Avci G, Yeşilada E, Bacak E (2010) Beneficial effects of *Aesculus hippocastanum* L. seed extract on the body's own antioxidant defense system on subacute administration. *J Ethnopharmacol* **129**: 18–22. doi: 10.1016/j.jep.2010.02.017.
- Lemar KM, Aon MA, Cortassa S, O'Rourke B, Müller CT, Lloyd D (2007) Diallyl disulphide depletes glutathione in *Candida albicans*: oxidative stress-mediated cell death studied by two-photon microscopy. *Yeast* **24**: 695–706. doi: 10.1002/yea.1503.
- Lemasters JJ (1999) Necrapoptosis and the mitochondrial permeability transition: shared pathways to necrosis and apoptosis. *Am J Physiol* **276**: G1–G6.
- Lindner I, Meier C, Url A, Unger H, Grassauer A, Prieschl-Grassauer E, Doerfler P (2010) Beta-escin has potent anti-allergic efficacy and reduces allergic airway inflammation. *BMC Immunol* **11**: 24. doi: 10.1186/1471-2172-11-24.
- Ly JD, Grubb DR, Lawen A (2003) The mitochondrial membrane potential ($\Delta\psi_m$) in apoptosis; an update. *Apoptosis* **8**: 115–128. doi: 10.1023/A:1022945107762.
- Mari M, Morales A, Colell A, García-Ruiz C, Kaplowitz N, Fernández-Checa JC (2013) Mitochondrial glutathione: features, regulation and role in disease. *Biochim Biophys Acta* **1830**: 3317–3328. doi: 10.1016/j.bbagen.2012.10.018.
- Matés JM, Segura JA, Alonso FJ, Márquez J (2012) Oxidative stress in apoptosis and cancer: an update. *Arch Toxicol* **86**: 1649–1665. doi: 10.1007/s00204-012-0906-3.
- Mela L, Seitz S (1979) Isolation of mitochondria with emphasis on heart mitochondria from small amounts of tissue. *Enzymol Meth* **55**: 39–46. doi:10.1016/0076-6879(79)55006-X.
- Mojžišová G, Mojžiš J, Pilátová M, Varinská L, Ivanová L, Strojný L, Richnavský J (2013) Antiproliferative and antiangiogenic properties of horse chestnut extract. *Phytother Res* **27**: 159–165. doi: 10.1002/ptr.4688.
- Mosman, T (1983) Rapid colorimetric assay for cellular growth and survival: application to proliferation and cytotoxicity assays. *J Immunol Methods* **65**: 55–63. doi:10.1016/0022-1759(83)90303-4.
- Nagata S (2000) Apoptotic DNA fragmentation. *Exp Cell Res* **256**: 12–18. doi:10.1006/excr.2000.4834.
- Nemoto S, Takeda K, Yu ZX, Ferrans VJ, Finkel T (2000) Role for mitochondrial oxidants as regulators of cellular metabolism. *Mol Cell Biol* **20**: 7311–7318. doi: 10.1128/MCB.20.19.7311-7318.2000.
- Niu YP, Li LD, Wu LM (2008) Beta-aescin: A potent natural inhibitor of proliferation and inducer of apoptosis in human chronic myeloid leukemia K562 cells *in vitro*. *Leuk Lymphoma* **29**: 1–8. doi: 10.1080/10428190802090151.
- Okon IS, Zou MH (2015) Mitochondrial ROS and cancer drug resistance: Implications for therapy. *Pharmacol Res* **100**: 170–174. doi: 10.1016/j.phrs.2015.06.013.
- Olszewska A, Szweczyk A (2013) Mitochondria as a pharmacological target: Magnum overview. *IUBMB Life* **65**: 273–281. doi: 10.1002/iub.1147.
- Ong PL, Weng BC, Lu FJ, Lin ML, Chang TT, Hung RP, Chen CH (2008) The anticancer effect of protein-extract from *Bidens alba* in human colorectal carcinoma SW480 cells *via* the reactive oxidative species- and glutathione depletion-dependent apoptosis. *Food Chem Toxicol* **46**: 1535–1547. doi: 10.1016/j.fct.2007.12.015.
- Parsons M, Green DR (2010) Mitochondria in cell death. *Essays Biochem* **47**: 99–114. doi: 10.1042/bse0470099.
- Patlolla JMR, Raju J, Swamy MV, Rao CHV (2006) β -Escin inhibits colonic aberrant crypt foci formation in rats and regulates the cell cycle growth by inducing p21^{waf1/cip1} in colon cancer cells. *Mol Cancer Ther* **5**: 1459–1466. doi: 10.1158/1535-7163.MCT-05-0495.
- Petit PX, Gendron MC, Schrantz N, Métivier D, Kroemer G, Maciorowska Z, Sureau F, Koester S (2001) Oxidation of pyridine nucleotides during Fas- and ceramide-induced apoptosis in Jurkat cells: correlation with changes in mitochondria, glutathione depletion, intracellular acidification and caspase 3 activation. *Biochem J* **353**: 357–367. doi: 10.1042/bj3530357.
- Pittler MH, Ernst E (2012) Horse-chestnut seed extract for chronic venous insufficiency. *Cochrane Database Syst Rev* **25**: CD 003230. doi: 10.1002/14651858.CD003230.pub4.
- Pogue BW, Pitts JD, Mycek MA, Sloboda RD, Wilmot CM, Brandsema JF, O'Hara JA (2001) *In vivo* NADH fluorescence monitoring as an assay for cellular damage in photodynamic therapy. *Photochem Photobiol* **74**: 817–824. doi: 10.1562/0031-8655(2001)0740817IVNF-MA2.0.CO2.
- Rimmon A, Vexler A, Berkovich L, Earon G, Ron I, Lev-Ari S (2013) Escin chemosensitizes human pancreatic cancer cells and inhibits the nuclear factor-kappaB signaling pathway. *Biochem Res Int* **2013**: 251752. doi.org/10.1155/2013/251752.
- Shen DY, Kang JH, Song W, Zhang WQ, Li WG, Zhao Y, Chen QX (2011) Apoptosis of human cholangiocarcinoma cell lines induced by β -escin through mitochondrial caspase-dependent pathway. *Phytother Res* **25**: 1519–1526. doi: 10.1002/ptr.3435.
- Shishodia S, Aggarwal BB (2004) Nuclear factor-kappaB activation mediates cellular transformation, proliferation, invasion angiogenesis and metastasis of cancer. *Cancer Treat Res* **119**: 139–173. doi: 10.1007/1-4020-7847-1_8.
- Sirtori CR (2001) Aescin: Pharmacology, pharmacokinetics and therapeutic profile. *Pharmacol Res* **44**: 183–193. doi:10.1006/phrs.2001.0847.
- Suter A, Bommer S, Rechner J (2006) Treatment of patients with venous insufficiency with fresh plant horse chestnut seed extract: a review of 5 clinical studies. *Adv Ther* **23**: 179–190. doi:10.1007/BF02850359.
- Tepe B, Tuncer E, Saraydn SU, Ozer H, Sen M, Karadayi K, Inan DS, Karadayi S, Polat Z, Akpulat A, Duman M, Koksall B, Turan M (2013) Antitumoral effects of *Allium sivasianum* on breast cancer in vitro and in vivo. *Mol Biol Rep* **40**: 597–604. doi: 10.1007/s11033-012-2098-6.
- Tomečková V, Štefanišinová M, Bilecová-Rabajdová M, Křiššáková E, Tomečko M, Tóth Š, Pekárová T, Mareková M (2011) A novel method for the detection of liver damage using fluorescence of hepatic mitochondria in a rat model following ischaemia/reperfusion injury of the small intestine. *Spectroscopy* **26**: 237–243. doi: 10.3233/SPE-2011-0545.
- Vidinský B, Gál P, Pilátová M, Vidová Z, Solár P, Varinská L, Ivanová L, Mojžiš J (2012) Anti-proliferative and anti-angiogenic effects of CB2R agonist (JWH-133) in non-small lung cancer cells (A549) and human umbilical vein endothelial cells: an *in vitro* investigation. *Folia Biol (Praha)* **58**: 75–80.
- Wang Q, Kuang H, Su Y, Sun Y, Feng J, Guo R, Chan K (2013) Naturally derived anti-inflammatory compounds from Chinese medicinal plants. *J Ethnopharmacol* **146**: 9–39. doi: 10.1016/j.jep.2012.12.013.
- Wang YW, Wang SJ, Zhou YN, Pan SH, Sun B (2012) Escin augments the efficacy of gemcitabine through down-regulation of nuclear factor- κ B and nuclear factor- κ B-regulated gene products in pancreatic cancer both *in vitro* and *in vivo*. *J Cancer Res Clin Oncol* **138**: 785–797. doi: 10.1007/s00432-012-1152-z.
- Wu H, Che X, Zheng Q, Wu A, Pan K, Shao A, Wu Q, Zhang J, Hong Y (2014) Caspases: a molecular switch node in the crosstalk between autophagy and apoptosis. *Int J Biol Sci* **10**: 1072–1083. doi:10.7150/ijbs.9719.
- Zhang X, Yuan L, Yang XW, Jiao SY, Wang Q (2010) Oxidative mechanism for toxicity induced by sodium aescinate in HK-2 cells. *Chin J Pharmacol Toxicol* **24**: 471–475. doi: 10.3867/j.issn.1000-3002.2010.06.005.
- Zhang Z, Gao J, Cai X, Zhao Y, Wang Y, Lu W, Gu Z, Zhang S, Cao P (2011) Escin sodium induces apoptosis of human acute leukemia Jurkat T cells. *Phytother Res* **25**: 1747–1755. doi: 10.1002/ptr.3457.
- Zhou XY, Fu FH, Li Z, Dong QJ, He J, Wang CH (2009) Escin a natural mixture of triterpene saponins exhibits antitumor activity against hepatocellular carcinoma. *Planta Med* **75**: 1580–1585. doi: 10.1055/s-0029-1185838.